Chemical Science

ROYAL SOCIETY OF CHEMISTRY

EDGE ARTICLE

View Article Online
View Journal | View Issue

Check for updates

Cite this: *Chem. Sci.*, 2025, **16**, 16225

All publication charges for this article have been paid for by the Royal Society of Chemistry

A scalable zinc-based coordination network for energy-efficient NF_3/CF_4 separation with unprecedented selectivity

Yi-Tao Li,†[a] Weilin Li,†[b] Li-Ping Zhang,[a] Na Geng,[c] Li Xu,[a] Shao-Min Wang,[a] Tingyu Zhu,[c] Qingqing Guan,*[d] Yangyang Guo,*[c] Xingxing Li *[b] and Qing-Yuan Yang *[a]

Received 5th July 2025
Accepted 5th August 2025

DOI: 10.1039/d5sc04966k

rsc.li/chemical-science

Nitrogen trifluoride (NF_3) and carbon tetrafluoride (CF_4) are critical gases in the semiconductor industry. However, their current lack of effective recycling and separation results in significant waste emissions, which are not only costly but also pose significant environmental challenges. Their separation remains a critical challenge due to their nearly identical physicochemical properties (Δbp <1 °C, similar polarizability). Here, we demonstrate that a zinc-based metal–organic framework (CALF-20) with precisely tuned 4.8 Å pores achieves exceptional NF_3/CF_4 separation through molecular sieving. At 298 K, this material exhibits a record-high NF_3/CF_4 adsorption ratio of 41.1, and a CF_4 purity of 99.5% can be achieved through breakthrough experiments. Structural characterization and computational studies reveal that the unique pore channel properties preferentially adsorb NF_3 (kinetic diameter: 4.5 Å) while effectively excluding CF_4 (4.8 Å). This advance enables cost-effective gas purification at $12.3 per kilogram, providing a practical solution for sustainable semiconductor manufacturing.

Introduction

Following a decade of advancement, the global semiconductor market is projected to attain a valuation of one trillion dollars by the year 2030.[1] Fluorinated electronic specialty gases, including NF_3, CF_4 and other fluorinated gases, play an essential role in contemporary semiconductor manufacturing due to their distinctive chemical reactivity during plasma etching and cleaning processes.[2,3] However, the semiconductor industry, which serves as a fundamental component of the global digital economy, is confronted with a growing environmental dilemma. The fluorinated process gases critical to semiconductor manufacturing – nitrogen trifluoride (NF_3) and carbon tetrafluoride (CF_4) – exhibit extraordinarily high global warming potentials (GWPs) of 17 200 and 6500 CO_2-equivalent, respectively, with atmospheric lifetimes of 740 years for NF_3 and 50 000 years for CF_4.[4,5] In the semiconductor manufacturing process, only a small portion of fluorinated gases are fully utilized, and a large amount of CF_4 and NF_3 exhaust gases remain stable after etching and cleaning, requiring high-temperature combustion or thermal plasma decomposition to effectively remove them.[6] Despite the treatment of exhaust gases, these trace amounts of fluorine-containing compounds inevitably escape into the atmosphere through ventilation systems.[7] The emissions of fluorinated gases from the global semiconductor industry are experiencing a year-on-year increase, which poses a considerable threat to the environment.[8,9] The separation and recycling of NF_3 and CF_4 through advanced separation technologies not only enable their efficient recovery for industrial reuse—significantly reducing operational costs—but also promote optimal resource utilization. Importantly, this approach significantly mitigates F-gas emissions, substantially diminishing their environmental impact.

Current industrial recovery of fluorinated gases predominantly relies on cryogenic distillation and liquefaction techniques, which operate under energetically demanding high-pressure and low-temperature conditions.[10,11] Porous adsorbent-based separation has emerged as an energy-efficient and economically viable strategy for the enrichment and recovery of high-value specialty gases. Porous materials—including zeolites,[12] activated carbons,[13–15] metal–organic frameworks (MOFs),[16,17] and porous organic cages—have demonstrated potential for fluorinated gas (F-gas) separation.

---

[a] State Key Laboratory of Fluorine & Nitrogen Chemicals, National Innovation Platform (Center) for Industry-Education Integration of Energy Storage Technology, School of Chemical Engineering and Technology, Xi'an Jiaotong University, Xi'an, 710049, China. E-mail: qingyuan.yang@xjtu.edu.cn

[b] Hefei National Research Center for Physical Sciences at the Microscale, University of Science and Technology of China, Anhui, 230026, China. E-mail: lixx@ustc.edu.cn

[c] CAS Key Laboratory of Green Process and Engineering, Institute of Process Engineering, Chinese Academy of Sciences, Beijing 100190, China. E-mail: yyguo@ipe.ac.cn

[d] Key Laboratory of Oil and Gas Fine Chemicals of Ministry of Education, College of Chemical Engineering, Xinjiang University, Urumqi 830017, China. E-mail: guanqq@xju.edu.cn

† Y. T. Li and W. L. Li contributed equally to this work.

However, while numerous traditional porous materials have been investigated for NF_3/N_2 and CF_4/N_2 separation, most reported adsorbents demonstrate limited selectivity for NF_3/CF_4. The separation of NF_3 and CF_4 remains a significant challenge in gas purification due to their nearly identical kinetic diameters. The urgency to address this challenge is further emphasized by the pledge of the semiconductor industry to achieve net-zero emissions by 2050.[18] This imperative demands the development of advanced materials that can effectively balance industrial scalability requirements with the need for molecular-level precision (Scheme 1).

MOFs have emerged as highly efficient adsorbents for gas separation, offering tunable pore geometries and chemical functionalities.[19] Recent advances in ultra-microporous MOFs (pore size <7 Å) demonstrate exceptional selectivity for fluorinated gases (F-gases) *via* size exclusion and host–guest interactions. For instance, amino-functionalized NH_2–Ni-MOF achieves a CF_4/N_2 selectivity of 46.3 through optimized van der Waals interactions,[20] while Co-MOF-74 exhibits NF_3/N_2 selectivity of 299.6 *via* Lewis acid–base interactions at open metal sites.[21] Although some MOF materials have exhibited favorable performance in separating specific fluorinated gases, no MOF material has currently achieved effective sieving of NF_3/CF_4. This is primarily due to the critical limitations inherent in MOF materials: (1) pore collapse during F-gas adsorption (*e.g.*, the M-MOF-74 series), whereas CALF-20 maintains high stability in both five cycles of static NF_3 adsorption and dynamic breakthrough experiments; (2) the failure of previous adsorbents to discriminate between NF_3 and CF_4 during adsorption processes, in contrast to CALF-20, which exhibits a record-high NF_3/CF_4 adsorption ratio of 41.1; (3) synthetic complexity that hinders scale-up, while CALF-20 is the first MOF material produced on an industrial scale. Achieving simultaneous high selectivity, structural stability, and industrial viability remains a long-standing challenge.

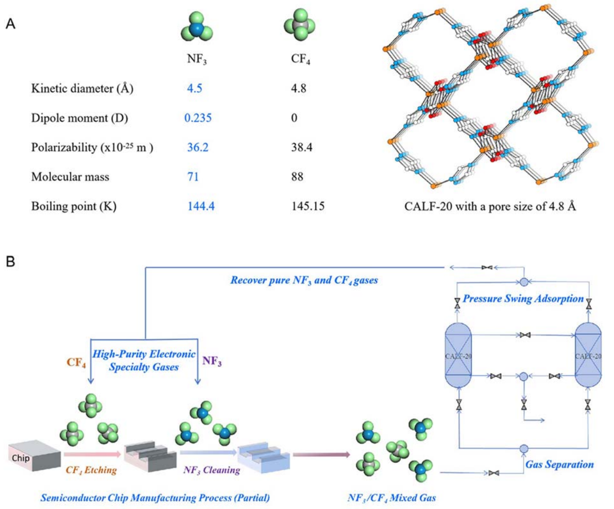

Scheme 1 (A) A comparison of some physical parameters of NF_3 and CF_4 and the pore structure of CALF-20. (B) The NF_3/CF_4 mixture in semiconductor manufacturing is efficiently separated, purified, and recycled through a pressure swing adsorption (PSA) device packed with CALF-20.

Extensive research suggests that realizing efficient NF_3/CF_4 separation necessitates MOF materials with meticulously tailored pore dimensions and the exclusion of open metal sites. These rigorous specifications substantially narrow the scope of candidate materials. When stability requirements and cost considerations are additionally factored in, CALF-20 emerges as the most promising viable option currently available. The separation of NF_3 and CF_4, key fluorinated gases in semiconductor manufacturing, poses a significant challenge due to their similar kinetic diameters. Despite extensive research on MOFs as potential adsorbents for gas separation, achieving efficient NF_3/CF_4 separation remains elusive. Existing MOF materials either lack the precise pore sizes required for molecular sieving or suffer from poor recyclability under industrial conditions, with many frameworks experiencing structural degradation after repeated adsorption cycles.

To address these limitations, this study focuses on developing scalable MOF adsorbents capable of molecular discrimination and practical recyclabilityfor NF_3/CF_4 separation. Herein, we introduce CALF-20, an industrially viable MOF engineered with precisely tuned 4.8 Å ultra-micropores. By utilizing steric exclusion effects, CALF-20 is designed to overcome the long-standing challenge of separating NF_3 and CF_4. Notably, this material exhibits a record-high NF_3/CF_4 selectivity of 41.1 and achieves >99.5% CF_4 purity in breakthrough experiments.

This work not only proposes a material design strategy for targeted gas separation but also demonstrates the potential of CALF-20 in enabling the recovery of NF_3 and CF_4 through PSA systems. Such an approach offers a sustainable pathway for the energy-efficient recovery of fluorinated gases, in line with the goal of the semiconductor industry to achieve net-zero emissions by 2050.[22]

Results and discussion

Adsorption performance of CALF-20 for NF_3

CALF-20 is constructed from zinc(II) ion layers interconnected by 1,2,4-triazole ligands and oxalate ion ligand pillars.[23] In recent years, numerous studies on gas separation systems related to CALF-20 have been published,[24–26] and we have also explored its adsorption properties.[27,28] However, there has been no prior report on CALF-20 for the adsorption of NF_3 and CF_4. This study represents the first investigation into the adsorption and separation performance of CALF-20 for NF_3/CF_4. As a robust adsorbent for NF_3 capture, CALF-20 demonstrates exceptional structural integrity and cycling stability under various operational conditions (Fig. 1). The temperature-dependent adsorption isotherms (273–313 K) reveal a characteristic Type I physisorption behavior, with NF_3 uptake capacity increasing systematically from 32.1 $cm^3\ g^{-1}$ at 313 K to 51.1 $cm^3\ g^{-1}$ at 273 K, following expected thermodynamic trends (Fig. 1A). Remarkably, five consecutive adsorption–desorption cycles at 298 K (Fig. 1B) show outstanding reproducibility, with NF_3 working capacity maintained at 37.4 ± 0.7 $cm^3\ g^{-1}$ (variation

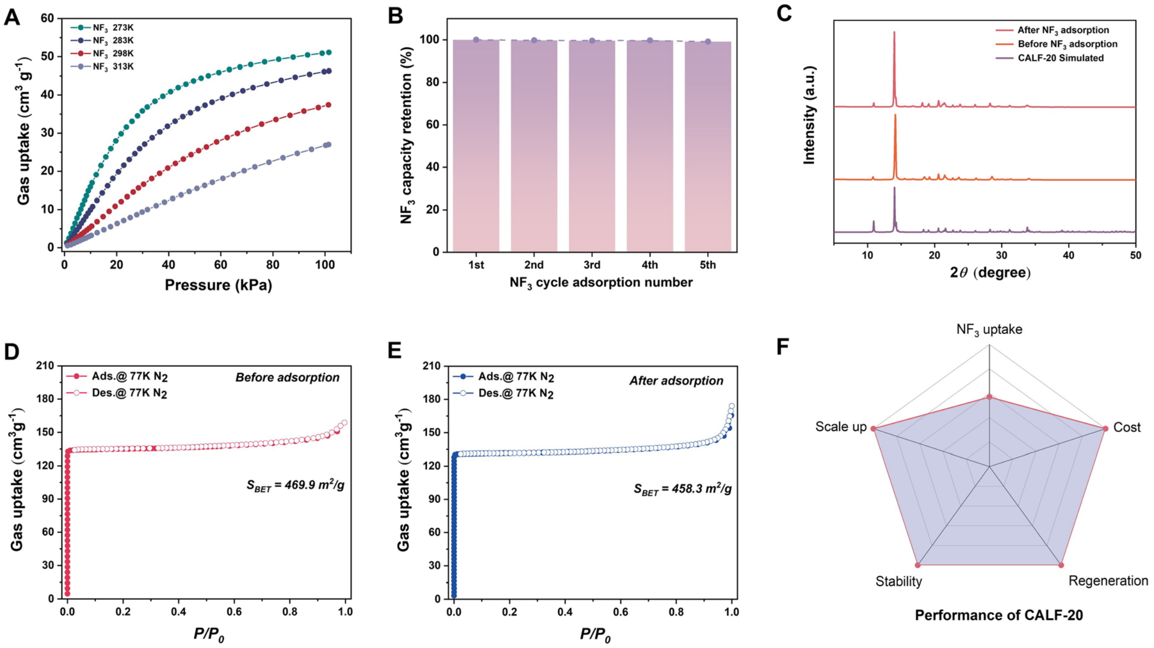

Fig. 1 Adsorption properties and cycling stability of CALF-20 for NF_3 capture. (A) The NF_3 adsorption isotherms on CALF-20 at different temperatures. (B) Capacity retention performance of NF_3 cycle adsorption. (C) The PXRD pattern of CALF-20 before and after NF_3 adsorption. (D) The N_2 sorption isotherms at 77 K before NF_3 adsorption. (E) The N_2 sorption isotherms at 77 K after NF_3 adsorption. (F) The five-criteria radar chart of the CALF-20.

<2%), demonstrating excellent cycling stability that meets industrial requirements for long-term operation. Notably, CALF-20 demonstrates exceptional stability toward NF_3 – a unique characteristic unmatched by other MOF materials. To our knowledge, it represents the first MOF capable of maintaining consistent NF_3 adsorption performance through multiple cycles without observable performance degradation. Comprehensive characterization further confirms the structural robustness of the framework. The PXRD patterns (Fig. 1C) display identical peak positions and intensities both before and after NF_3 exposure. There is no observable peak broadening, and no new phases emerge, which indicates that the crystallinity is completely retained. N_2 physisorption measurements (Fig. 1D and E) show minimal changes in porosity, with BET surface area decreasing only slightly from 467 m^2 g^{-1} to 458 m^2 g^{-1} (<2.5% reduction) and pore volume remaining essentially unchanged (0.38 cm^3 g^{-1} *vs.* 0.37 cm^3 g^{-1}), suggesting negligible pore damage or structural collapse. These results are supplemented by a five-dimensional performance evaluation (Fig. 1F) that quantitatively assesses the balanced characteristics of CALF-20, including its high NF_3 uptake capacity (performance), excellent cycling stability (stability), mild regeneration conditions (regeneration), scalable synthesis (cost), and wide operating temperature range (scale up).

The combined evidence from these systematic characterizations establishes CALF-20 as a structurally durable and practically viable adsorbent for industrial NF_3 separation processes, offering significant advantages over traditional materials in terms of both performance and operational stability. The ability of the material to maintain its adsorption capacity and structural integrity under repeated cycling, coupled with its temperature-dependent tunability, positions it as a promising candidate for pressure-swing adsorption applications in fluorocarbon purification.

Molecular sieving for efficient NF_3/CF_4 separation

CALF-20 exhibited negligible adsorption of CF_4 across the temperature range of 273–313 K. Adsorption isotherms at 298 K establish CALF-20 as a near-ideal molecular sieve, exhibiting complete exclusion of CF_4 (uptake <1 cm^3 g^{-1}) while achieving suitable NF_3 capacity (37.4 cm^3 g^{-1} at 100 kPa) (Fig. 2A). Our study reveals that CALF-20 exhibits unique temperature-dependent molecular sieving properties. Across a broad temperature range (273–313 K), the material consistently demonstrates complete exclusion of CF_4 while maintaining stable NF_3 uptake (Fig. 2B). A moderate temperature decrease from 298 K to 273 K at 100 kPa does not significantly increase CF_4 adsorption capacity, but significantly enhances NF_3 adsorption capacity to 51.1 cm^3 g^{-1}, representing an increase of approximately 36.6% compared to the uptake at 298 K (Fig. 2C).

CALF-20 exhibits an exceptional NF_3/CF_4 adsorption ratio of 41.1 at 298 K (Fig. 2D), significantly surpassing all the previously reported porous materials including ATC-Cu (1.46),[29] HKUST-1 (1.18),[20] $Cu(peba)_2$ (1.07),[20] $Ni(pba)_2$ (0.83),[20] Ni-MOF (0.91),[20] NH_2–Ni-MOF (1.08),[20] $Co_3(HCOO)_6$ (1.03),[30] $Ni_3(HCOO)_6$ (1.33),[30] $Mn_3(HCOO)_6$ (1.84)[30] and SBMOF-1 (1.16).[31] This outstanding separation performance is of great significance in the field of fluorocarbon separation, as it can potentially revolutionize the industrial separation processes of NF_3/CF_4 mixtures, reducing energy consumption and improving separation efficiency. This

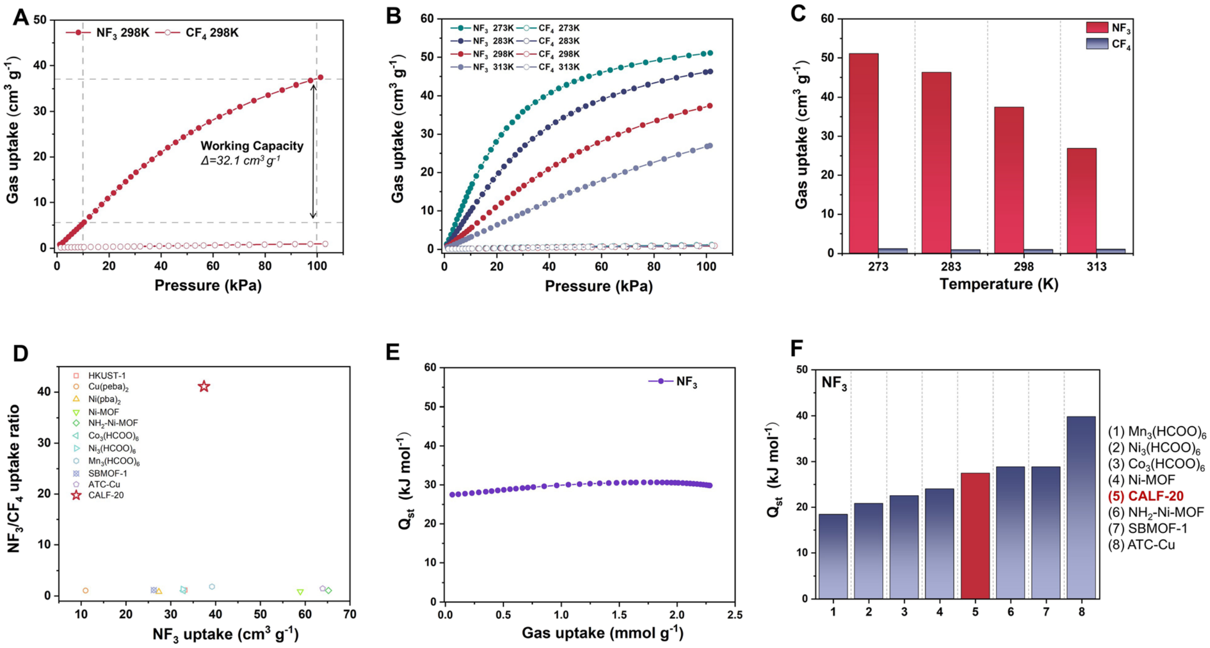

Fig. 2 Molecular sieving and thermodynamic analysis of NF_3/CF_4 separation in CALF-20. (A) The NF_3 and CF_4 adsorption isotherms of CALF-20 at 298 K. (B) The NF_3 and CF_4 adsorption isotherms of CALF-20 at different temperatures. (C) Adsorption capacity of CALF-20 for NF_3 and CF_4 at 100 kPa and different temperatures. (D) NF_3 uptakes and NF_3/CF_4 uptake ratio comparison with some reported materials at 298 K and 100 kPa. (E) Isosteric heats of adsorption (Q_{st}) of NF_3. (F) The calculated NF_3 Q_{st} of CALF-20 and other reported materials.

remarkable enhancement in separation performance demonstrates the unique molecular sieving capability of CALF-20 for NF_3/CF_4 mixtures. While other MOFs show adsorption ratios clustered near the vapor–liquid equilibrium prediction (~1.25), CALF-20 achieves a 28-fold improvement over the previous best performer (ATC-Cu), establishing new benchmarks for fluorocarbon separations. The superior performance originates from the precisely tuned pore structure of CALF-20. This pore structure enables complete exclusion of CF_4 while maintaining an effective NF_3 adsorption capacity. The isosteric heat of adsorption (Q_{st}) for NF_3 in CALF-20 was determined to be 27.5 kJ mol^{-1} at zero coverage (Fig. 2E), calculated from gas adsorption isotherms over 273–313 K. This intermediate binding strength represents an optimal balance for practical applications: sufficiently strong to ensure effective NF_3 capture at ambient conditions, yet weak enough to permit energy-efficient regeneration (Fig. 2F). Compared with other materials, this unique adsorption energy characteristic endows CALF-20 with distinct advantages in terms of adsorption efficiency and regeneration performance, which is crucial for its large-scale industrial application.

Diffusion barriers and host–guest interactions of NF_3/CF_4 in CALF-20

Minimum energy path (MEP) calculations reveal fundamentally different diffusion mechanisms for NF_3 and CF_4 during adsorption in the channels of CALF-20. The energy profile shows that NF_3 encounters a moderate activation barrier of 65.6 kJ mol^{-1} at the channel bottleneck (position-6, Fig. 3A and B), while CF_4 faces a substantially higher barrier of 111.7 kJ mol^{-1} (position-5, Fig. 3D and E) – consistent with its larger kinetic diameter (4.8 Å *vs.* 4.5 Å for NF_3). Furthermore, an analysis of host–guest interaction distances reveals that CF_4 exhibits stronger interactions (H⋯F: 2.60–3.69 Å) compared to NF_3 (H⋯F: 2.64–4.03 Å) (Fig. S5), which underscores the steric hindrance associated with its molecular structure.

Synergistic analysis of breakthrough experiments and *in situ* infrared spectroscopy

The separation mechanism is synergistically verified by combining the macroscopic separation performance from breakthrough experiments with the microscopic interaction mechanism revealed by *in situ* infrared spectroscopy. In order to evaluate the separation capabilities of CALF-20 for NF_3/CF_4 mixtures, we conducted dynamic breakthrough experiments at a temperature of 298 K utilizing an equimolar (50/50, v/v) NF_3/CF_4 gas mixture. The gas was introduced at a flow rate of 6 mL min^{-1} through a packed column filled with the activated adsorbent. Breakthrough experiments reveal instantaneous CF_4 permeation (retention time = 1.3 min g^{-1}) *versus* strong NF_3 retention (5.3 min g^{-1}) in CALF-20, demonstrating its molecular sieving selectivity for NF_3/CF_4 separations (Fig. 4A). Five consecutive breakthrough cycles demonstrate the stable NF_3/CF_4 separation performance of CALF-20. The retention times are nearly identical, which confirms the recyclability of CALF-20 for industrial gas purification (Fig. 4B). Temperature-dependent breakthrough measurements reveal enhanced NF_3/CF_4 separation at 273 K and 283 K, with NF_3 retention time increasing by

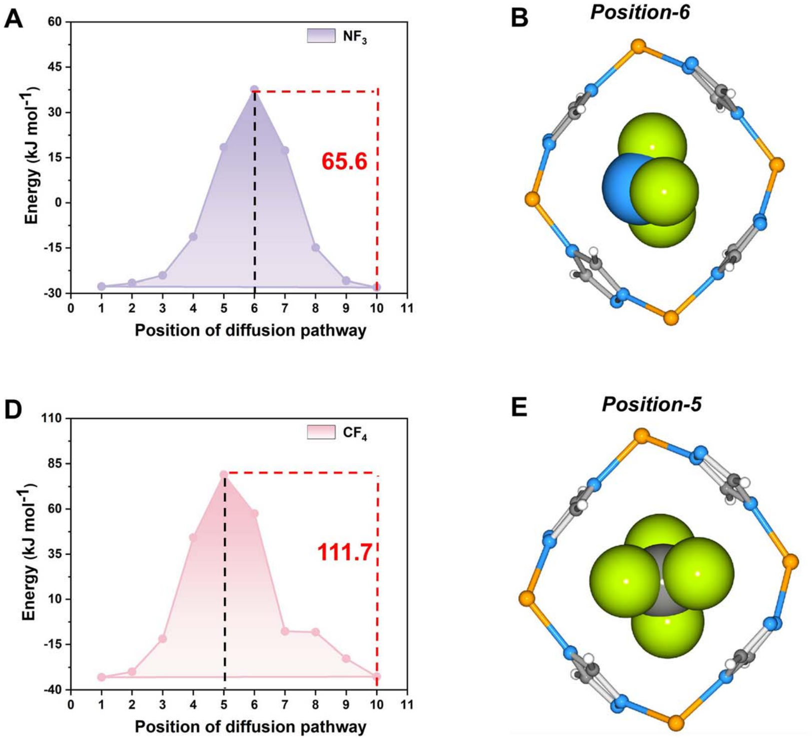

Fig. 3 DFT calculations. Energy profiles for NF_3 (A) and CF_4 (D) diffusion in CALF-20; molecular configuration at the positions with maximum energy for NF_3 (B and C) and CF_4 (E and F) in CALF-20.

52% and 96% (from 5.3 to 8.1 and 10.2 min g^{-1}) while maintaining the instantaneous permeation of CF_4, indicating that reducing the temperature appropriately will not significantly increase energy consumption, but will significantly enhance the separation performance of NF_3/CF_4 (Fig. 4C). Regeneration studies at 298 K using He purge gas (6 mL min^{-1}) revealed

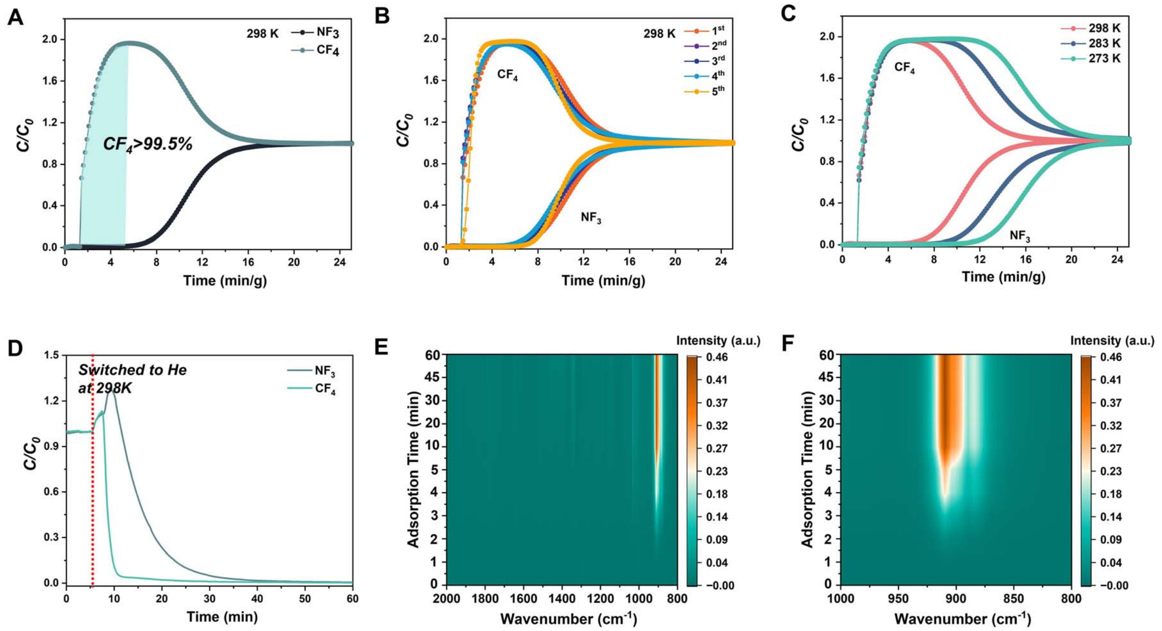

Fig. 4 The breakthrough performance and *in situ* infrared spectroscopy of CALF-20. (A) The NF_3/CF_4 breakthrough curve of CALF-20 at 298 K (adsorption condition: NF_3/CF_4 v/v 50/50 with the flow rate of 6 mL min^{-1}). (B) Five cycles of column breakthrough experiments. (C) The NF_3/CF_4 breakthrough curves of CALF-20 at different temperatures. (D) Desorption curves by He purge with the flow rate of 6 mL min^{-1} at 298 K. (E) *In situ* 3D DRIFTS spectral mapping of 1% NF_3 adsorption on CALF-20 from 0–60 min. (F) *In situ* DRIFTS mapping showing localized N–F bond perturbations (910 cm^{-1}).

distinct desorption kinetics where CF_4 was rapidly eluted, while NF_3 exhibited prolonged retention. This directly demonstrates that CALF-20 had a stronger affinity for NF_3 at room temperature (Fig. 4D). To investigate the interaction mechanism between NF_3 and CALF-20, we employed *in situ* FTIR spectrum to monitor real-time vibrational changes during NF_3 adsorption. Within the 2000–800 cm^{-1} range, the FTIR spectrum exhibited only the N–F asymmetric stretching vibration of NF_3 at 910 cm^{-1} (Fig. 4E). *In situ* FTIR spectroscopy of NF_3 adsorbed in CALF-20 exhibited an unshifted N–F asymmetric stretching vibration at 910 cm^{-1} (Fig. 4F), which is identical to the infrared resonance peak reported in the references for pure NF_3 gas measurements.[32] This observation suggests that the interaction between NF_3 and CALF-20 is weak and primarily governed by physisorption. Besides, the 3D DRIFTS spectra recorded during desorption (Fig. S6) showed a symmetric decrease in the 910 cm^{-1} band intensity, mirroring the adsorption profile and confirming the reversibility of NF_3 uptake—an essential attribute for practical PSA applications. This reversibility, coupled with the sustained framework integrity (no new peaks or shifts in XRD patterns during multiple adsorption–desorption cycles), further underscores the structural stability of CALF-20 under operational conditions.

Combining the different diffusion energy barriers obtained from our DFT calculations (65.6 kJ mol^{-1} *vs.* 111.7 kJ mol^{-1}) and breakthrough data demonstrating high NF_3/CF_4 selectivity, we conclude that molecular sieving in CALF-20 is governed primarily by sieving rather than differential adsorption affinity. The retention of the vibrational signature of NF_3 further confirms the structural stability of the framework during NF_3 gas uptake.

Conclusion

In summary, CALF-20, a metal–organic framework with precisely engineered 4.8 Å pores, has emerged as a breakthrough solution for the separation of nitrogen trifluoride (NF_3) and carbon tetrafluoride (CF_4) in semiconductor manufacturing. This material achieves an NF_3/CF_4 uptake ratio of 41.1 and can produce CF_4 with a purity of >99.5% through breakthrough experiments at 298 K, setting a new benchmark for fluorocarbon separation. The unique pore structure of CALF-20 enables selective molecular sieving of NF_3 (kinetic diameter: 4.5 Å) while effectively excluding CF_4 (4.8 Å), as confirmed by structural characterization and computational studies. The remarkable stability and recyclability of the framework over multiple adsorption cycles, combined with its mild regeneration conditions and scalable synthesis, position it as a practical and cost-effective choice for industrial gas purification. This work not only addresses a critical environmental and economic challenge in the semiconductor industry but also provides a model for developing advanced porous materials that can achieve high selectivity and stability for challenging gas separations. By providing a viable way for the energy-efficient recovery of electronic special gases, CALF-20 supports the transition of the semiconductor sector to sustainable practices and the goal of achieving net-zero emissions by 2050.

Author contributions

Q.-Y. Y. initiated and supervised the research. Q.-Y. Y. and Y.-T. L. designed the project and experiments. Y.-T. L. performed the adsorbents preparation and gas adsorption experiments. L.W.L. and L.X.X performed the simulated calculations. Y.-Y. G., T.-Y. Z. and N. G. performed in-situ infrared spectroscopy measurements. Q.-Q. G. provided financial support for the study. L.-P. Z., L. X., S.-M. W., and Q.-Y. Y. discussed the experimental results and provided valuable suggestions. Y.-T. L. wrote the manuscript. Q.-Y. Y. performed manuscript edits and revisions. All authors contribute to the final manuscript and the interpretation of the results.

Conflicts of interest

There are no conflicts to declare.

Data availability

Additional details regarding the experimental and calculation data are given in the SI, including *in situ* infrared purging data in Fig. S1–S6 and Table S1 and S2. See DOI: **https://doi.org/10.1039/d5sc04966k**.

Acknowledgements

Y.-T. L. and W. L. L. contributed equally to this work. This work was financially supported by the National Natural Science Foundation of China (No. 22371221) and the Youth Innovation Promotion Association of the Chinese Academy of Sciences (No. 2021044) and Beijing Nova Program (2024072).

References

1 E. Schmidt, AI, great power competition & national security, *Daedalus*, 2022, **151**, 288–298.
2 S. Raoux, T. Tanaka, M. Bhan, H. Ponnekanti, M. Seamons, T. Deacon, L.-Q. Xia, F. Pham, D. Silvetti and D. Cheung, Remote microwave plasma source for cleaning chemical vapor deposition chambers: Technology for reducing global warming gas emissions, *J. Vac. Sci. Technol. B*, 1999, **17**, 477–485.
3 M. B. Chang and J.-S. Chang, Abatement of PFCs from semiconductor manufacturing processes by nonthermal plasma technologies: A critical review, *Ind. Eng. Chem. Res.*, 2006, **45**, 4101–4109.
4 R. Joeri, L. David, C. Brian and R. Keywan, emissions levels required to limit warmint to below 2°C, *Nat. Clim. Change*, 2020, **3**, 405–412.
5 M. J. Prather and J. Hsu, NF_3, the greenhouse gas missing from Kyoto, *Geophys. Res. Lett.*, 2008, **35**, L12810.
6 B. A. Wofford, M. W. Jackson, C. Hartz and J. W. Bevan, Surface wave plasma abatement of CHF_3 and CF_4 containing semiconductor process emissions, *Environ. Sci. Technol.*, 1999, **33**, 1892–1897.

7 H. S. Kim, E. Y. Kim and P. S. Lee, Study of the enrichment of NF_3 waste gas using zeolite and polymeric membranes, *Sep. Purif. Technol.*, 2019, **220**, 1–7.

8 P. Purohit and L. Höglund-Isaksson, Global emissions of fluorinated greenhouse gases 2005–2050 with abatement potentials and costs, *Atmos. Chem. Phys.*, 2017, **17**, 2795–2816.

9 K. M. Stanley, D. Say, J. Mühle, C. M. Harth, P. B. Krummel, D. Young, S. J. O'Doherty, P. K. Salameh, P. G. Simmonds and R. F. Weiss, Increase in global emissions of HFC-23 despite near-total expected reductions, *Nat. Commun.*, 2020, **11**, 397.

10 C. Y. Chuah, Y. Lee and T.-H. Bae, Potential of adsorbents and membranes for SF_6 capture and recovery: A review, *Chem. Eng. J.*, 2021, **404**, 126577.

11 C.-F. O. Yang, S.-H. Kam, C.-H. Liu, J. Tzou and J.-L. Wang, Assessment of removal efficiency of perfluorocompounds (PFCs) in a semiconductor fabrication plant by gas chromatography, *Chemosphere*, 2009, **76**, 1273–1277.

12 S. Singh, F. H. Tezel and P. J. Harlick, Adsorption of tetrafluoromethane and nitrogen by various adsorbents, *Sep. Sci. Technol.*, 2002, **37**, 2763–2784.

13 W. Fu, J. Wang, Y. Shi, Y. Li, Z. Sui, L. Wang, Y. Wang and X. Xu, One-step self-activated carbon adsorbent with synergistic micropore-mesopore structure for exceptional SF_6/N_2 separation performance, *Carbon*, 2025, **232**, 119839.

14 W. Fu, J. Wang, Y. Li, Z. Sui and X. Xu, Investigation on the pore structure-performance relationship of porous carbon adsorbents for SF_6/N_2 separation via fine pore modulation, *Sep. Purif. Technol.*, 2024, **348**, 127788.

15 Y. Shi, J. Wang, W. Fu, Y. Li, Z. Sui and X. Xu, In-situ activated carbon adsorbents with tailored pore structures for efficient SF_6 capture and high-purity recovery, *Sep. Purif. Technol.*, 2025, **360**, 130978.

16 J. Li, Y. Chen, T. Ke, Y. Jin, R. Fan, G. Xu, L. Yang, Z. Zhang, Z. Bao, Q. Ren and Q. Yang, Efficient continuous SF_6/N_2 separation using low-cost and robust metal-organic frameworks composites, *Nat. Commun.*, 2025, **16**, 632.

17 S. M. Wang, X. T. Mu, H. R. Liu, S. T. Zheng and Q. Y. Yang, Pore-structure control in metal–organic frameworks (MOFs) for capture of the greenhouse gas SF_6 with record separation, *Angew. Chem., Int. Ed.*, 2022, **134**, e202207066.

18 F. Shahzad, Y. B. Zaied, M. A. Shahzad and F. Mahmood, Insights into the performance of green supply chain in the Chinese semiconductor industry, *Int. J. Prod. Econ.*, 2024, **273**, 109286.

19 K. Adil, Y. Belmabkhout, R. S. Pillai, A. Cadiau, P. M. Bhatt, A. H. Assen, G. Maurin and M. Eddaoudi, Gas/vapour separation using ultra-microporous metal–organic frameworks: insights into the structure/separation relationship, *Chem. Soc. Rev.*, 2017, **46**, 3402–3430.

20 S.-M. Wang, H.-L. Lan, G.-W. Guan and Q.-Y. Yang, Amino-functionalized microporous MOFs for capturing greenhouse gases CF_4 and NF_3 with record selectivity, *ACS Appl. Mater. Interfaces*, 2022, **14**, 40072–40081.

21 S.-M. Wang, Q. Zhang, Y.-T. Li, S.-C. Liu and Q.-Y. Yang, Destructive Adsorption of Nitrogen Trifluoride (NF3) Using M-MOF-74 with Open Metal Sites, *Chem Bio Eng.*, 2024, **1**, 535–540.

22 M.-T. Huang and P.-M. Zhai, Achieving Paris Agreement temperature goals requires carbon neutrality by middle century with far-reaching transitions in the whole society, *Adv. Clim. Change Res.*, 2021, **12**, 281–286.

23 J.-B. Lin, T. T. Nguyen, R. Vaidhyanathan, J. Burner, J. M. Taylor, H. Durekova, F. Akhtar, R. K. Mah, O. Ghaffari-Nik and S. Marx, A scalable metal-organic framework as a durable physisorbent for carbon dioxide capture, *Science*, 2021, **374**, 1464–1469.

24 X. Peng, L. Zhao, Y.-L. Peng, C. Deng, Y. H. Andaloussi, H. Pan, Y.-J. Tian, J.-S. Zou, R. Krishna, B. Liu, C. Deng, P. Xiao, C. Sun, M. J. Zaworotko, G. Chen and Z. Zhang, One-Step Ethylene Purification from a Seven-Component Cracking Gas Mixture with Sorbent-Sorbate Induced-Fit, *CCS Chem.*, 2025, **7**, 1054–1066.

25 X. Wang, T. Zhao, Y. Cai, Y. Zheng, Y. Chen and J. Gao, Reversed CO_2/C_2H_2 separation with ultrahigh carbon dioxide adsorption capacity in Zn-based pillared metal-organic frameworks, *J. Solid State Chem.*, 2023, **327**, 124280.

26 T. Wu, C. Yu, R. Krishna, Z. Qiu, H. Pan, P. Zhang, X. Suo, L. Yang, X. Cui and H. Xing, Porous materials with suitable pore size and dual-functional sites for benchmark one-step ethylene purification, *AIChE J.*, 2024, **70**, e18312.

27 Y.-T. Li, W. Li, L.-P. Zhang, L. Xu, S. Ni, Y. Jiang, X. Li and Q.-Y. Yang, Zinc-Based flexible coordination network for precise butane isomer sieving and low-carbon alkane recovery from oilfield associated gas, *Sep. Purif. Technol.*, 2025, **363**, 132018.

28 Y. T. Li, W. Li, L. P. Zhang, S. Ni, Y. Jiang, X. Li and Q. Y. Yang, Wide Temperature Sieving of n-Butene and iso-Butene by a Zinc-Based Coordination Network with Record Separation, *Adv. Funct. Mater.*, 2025, **35**, 2411951.

29 Z.-W. Fan, Y. Wang, J. Liu, Z.-T. Cheng, C. Wang and Z. Niu, Metal–Organic Framework-Based NF_3 Nanotrap for the Separation of NF_3 and CF_4, *ACS Appl. Mater. Interfaces*, 2024, **17**, 2349–2354.

30 Y. Wu, T. Yan, W. Zhang, S. Chen, Y. Fu, Z. Zhang and H. Ma, Adsorption interface-induced H⋯F charge transfer in ultramicroporous metal–organic frameworks for perfluorinated gas separation, *Ind. Eng. Chem. Res.*, 2022, **61**, 13603–13611.

31 Y. Wu, S. Wang, W. Zhang, S. Chen, Z. Zhang, B. Yang, S. Li and H. Ma, Enhancing perfluorinated electron specialty gases separation selectivity in ultra-microporous metal organic framework, *Sep. Purif. Technol.*, 2022, **289**, 120739.

32 A. Guber and U. Köhler, FTIR spectroscopy for the analysis of selected exhaust gas flows in silicon technology, *J. Mol. Struct.*, 1995, **348**, 209–212.